Journal of Nano- and Electronic Physics
Vol. **11** No 6, 06016(6pp) (2019)

Журнал нано- та електронної фізики
Том **11** № 6, 06016(6cc) (2019)

Photodetector Properties of Polyaniline/CuO Nanostructures Synthesized by Hydrothermal Technique

Ahmed M. Shano[1,*], Iftikhar M. Ali[2], Nabeel A. Bakr[3]

[1] *Bilad Alrafidain University College, Department of Radiological Techniques, Diyala, Iraq*
[2] *Department of Physics, College of Science, University of Baghdad, Baghdad, Iraq*
[3] *Department of Physics, College of Science, University of Diyala, Diyala, Iraq*

(Received 20 August 2019; revised manuscript received 01 December 2019; published online 13 December 2019)

In this work, pure and copper mixed oxide PAni nanofiber thin films are successfully synthesized on silicon substrates by hydrothermal method and spin coating technique at room temperature with thickness of about 325 nm. The structural, surface morphological, optical and photoconductivity properties have been investigated. The XRD results showed that PAni films have crystalline nature, CuO and PAni/CuO nanostructure composites are monoclinic polycrystalline structure. The FESEM images of PAni clearly indicate that it has nanofiber-like structure, whereas the CuO film has sponge-like shape. The surface morphology analysis of PAni/CuO composite shows that nanofiber caped with inorganic material which is CuO is a core-shell structure. Optical characterization shows that the direct electronic transition is allowed in the energy gap. The values of energy gap for PAni nanofibers and CuO are 3.98 eV and 5.29 eV respectively. The spectral response of PAni nanofibers, CuO and PAni/CuO composite was studied. The values of responsivity and quantum efficiency of PAni/CuO composite are larger than those for pure PAni nanofibers. One can conclude that with mixing, the sensitivity is higher than that without mixing and is found to be 220 %. PAni/CuO composite exhibits fast rise time of 0.32 s with full time of 0.41 s, while slow rise time of 0.67 s and 0.38 s was respectively observed for PAni nanofibers and CuO with full time of 3.32 s and 1.19 s.

Keywords: Polyaniline, Copper oxide, Hydrothermal method, Spin coating, Photoconductivity.

DOI: 10.21272/jnep.11(6).06016 PACS numbers: 73.50.Pz, 84.71.Mn

1. INTRODUCTION

In spite of many applications of the conducting polymers in "plastic electronics" and solar cells, many of the basic properties of these materials still remain not fully understood, among others their most characteristic property – the electrical conductivity and the charge transport in general. Through heavy doping, their conductivity can reach metallic values at room temperature. However, it is usually an increasing function of temperature like in semiconductors [1, 2]. Polyaniline is low cost and has stability. [3]. Copper oxide has many kinds of formula, such as cuprous oxide (Cu_2O) and cupric oxide (CuO) [3]. Both types are *p*-type semiconductors. The potential applications of copper oxides include solar cells [4]. CuO is monoclinic structure and has features such as low cost and thermal stability [5]. Hydrothermal synthesis method has been established for forming nanosized material with high crystallinity and low cost comparing with other techniques [6]. A sensor is a device that can measure a parameter of physical and change it to an electrical signal. It contains velocity, temperature and light [7]. The purpose of this work is focused on the synthesis of PAni nanofibers (NFs), CuO and PAni/CuO composite by hydrothermal technique and studies of the structural, surface morphological, optical and photoconductivity properties of films.

2. EXPERIMENTAL PROCEDURE

Aniline (Ani) monomer 99.5 %, ammonium peroxydisulfate (APS), HCL, copper (II) chloride ($CuCl_2.2H_2O$) and hexamine ($C_6H_{12}N_4$) made in New Delhi Co., India, were of analytical grade and used without further purification. Double-distilled water was used for sample preparation and characterization.

12.5 mM of monomer ANI were dissolved in 76 ml of distilled water and stirred with a magnetic stirrer for 10 min to form an identical solution. 0.24 M (APS) were also dissolved in 4 ml of distilled water and magnetically stirred for 10 min. Then the APS solution was added rapidly with drastic stirring and 1.4 ml of HCl was directly added dropwise to the above solution with continuous stirring. After that mixture was stirred for 15 min and transferred into a Teflon-lined stainless steel hydrothermal reactor. The hydrothermal reactor was sealed quickly and maintained at 120 °C for 5 h in a digital temperature-controlled oven. Then, the hydrothermal reactor was cooled to room temperature rapidly by placing it into an icy water bath. The precipitate was centrifuged and washed with water several times and finally with ethanol until the supernatant fluid was colorless. Finally, this solution was deposited on cleaned silicon substrates by using spin coating technique as follows: an excess amount of the PAni solution is firstly

* Ahmed_alaskari89@yahoo.com

dropped onto the substrate. The spin coater then rotates the substrate at a speed of around 1400-2100 rpm for 1 min in order to spread the fluid by centrifugal force. The angular velocity of substrate with the overlying solution gives increase gradually to eject the excess applied solution and only a thin film remains on the substrate. The thickness and surface morphology of the final film obtained from a particular material in a given solvent is highly reproducible with excellent uniformity on large areas.

0.1 M copper (II) chloride ($CuCl_2.2H_2O$) solution was dissolved in 50 ml distilled water with continuous stirring at room temperature for 10 min. 0.1 M solution of hexamine ($C_6H_{12}N_4$) in 50 ml distilled water was prepared with continuous stirring at room temperature for 10 min. $C_6H_{12}N_4$ solution was added dropwise to copper (II) chloride solution with continuous stirring at room temperature for 20 min. Final solution was transferred into a Teflon-lined stainless steel hydrothermal reactor. The hydrothermal reactor was sealed quickly and maintained at 160 °C for 5 h in a digital temperature-controlled oven. The hydrothermal reactor was cooled to room temperature naturally. The precipitate was filtered and washed with water several times and finally with acetone until the supernatant fluid was colorless and then dried at 50 °C in an oven. This precipitate was annealed in air atmosphere at a temperature of 400 °C for one hour and left in the furnace to reach room temperature after turning off the furnace to obtain CuO. 0.05 g of CuO were dissolved in 15 ml of distilled water and 15 ml ethanol, and then these solutions were put in ultrasonic bath for 2 h to be good dispersed. Finally, this solution was deposited on cleaned silicon substrates by using spin coating technique and used to prepare PAni/CuO composites.

PAni NFs were mixed with different concentrations of CuO. PAni/CuO composites were prepared by adding colloidal CuO with volume ratio 7 ml to 10 ml of colloidal polyaniline, then putting the mixture solutions in ultrasonic bath for 2 h to mix them properly. Finally, the mixed solutions were deposited on silicon substrate by using spin coating technique.

3. RESULTS AND DISCUSSION

3.1 XRD Analysis

Fig. 1 shows the XRD patterns of PAni NFs, CuO thin film and PAni/CuO composite. The XRD pattern of PAni NFs shows two peaks at $2\theta = 19°$, which correspond to (020) crystal planes of PAni NFs, and at 28.5° referred to silicon substrate, which is in agreement with other reports [1, 8]. The crystalline PAni was due to its nano-fiber form and planar nature of Banzenoid and Quinoid functional groups [8]. The crystallite size (D) estimated for plane (020) by Scherer's method [8]:

$$D = \frac{K\lambda}{\beta \cos\theta}, \quad (1)$$

where K is the constant equal to 0.9, λ is the wavelength of incident X-ray radiation (1.5406 Å for CuKα), β is the full width at half maximum of the peak (in rad) and θ is the Bragg diffraction angle. The crystallite size is found to be 9.2 nm. From the XRD pattern of CuO thin film, it can be noticed that the pattern exhibits diffraction peaks around $2\theta \sim 32^o$, 35^o, 38^o , 48^o, 53^o, 58^o , 61^o, 66^o, 67^o, 72^o and 75^o denoted to (110), $(\bar{1}11)$, (111), $(\bar{2}02)$, (020), (202), $(\bar{1}13)$, $(\bar{3}11)$, (113), (311) and $(\bar{2}22)$, preferred directions respectively, which is in agreement with the Joint Committee of Powder Diffraction Standards (JCPDS) card number 41-0254. The strongest peak occurs at $2\theta \sim 35^o$ which is referred to $(\bar{1}11)$ plane. The positions of the peaks and the presence of more than one diffraction peak lead to the conclusion that the films are polycrystalline in nature with a monoclinic crystalline structure. It can be also noticed that the lattice constants a, b and c for CuO film are 4.692, 3.41 and 5.134 Å respectively as shown in Table 1 which indicates that the prepared film has the nearest values (a, b and c) to the standard lattice constants 4.685, 3.423 and 5.132 Å respectively. The average crystallite size of the film was estimated by Eq. (1) and it was found to be ~ 21 nm which is in agreement with other reports [9, 10] as shown in Table 1. The XRD pattern of PAni/CuO composite shows that the films are polycrystalline in nature with monoclinic structure and it can be noticed that the pattern exhibits diffraction peaks around $2\theta \sim 19°$, 35°, 38° and 47° referred to (020), $(\bar{1}11)$, (111) and $(\bar{2}02)$ preferred directions respectively. The diffraction peaks $(\bar{1}11)$, (111) and $(\bar{2}02)$ are referred to CuO and the peak (020) refers to PAni NFs [8]. It can be noticed also that the lattice constants a, b and c and crystallite size of PAni/CuO composite are larger than those for pure CuO and PAni NFs which is in agreement with other studies [11].

3.2 FESEM

Fig. 2 shows the scanning electron microscopy FESEM micrographs of PAni NFs, CuO nanostructure and PAni/CuO composite. Fig. 2a shows the FESEM image of the dense mesh PAni nanofiber films. The FESEM image of polyaniline clearly indicates that this polymer possesses nanofiber like structure. This image also reveals that PAni contains several voids or pores [12]. As shown from FESEM micrograph of nanocrystalline CuO thin film (Fig. 2b), a random distribution of CuO nanocrystallites over the scanned area can be observed and sponge-like shapes can be clearly noticed. Due to high surface charge, agglomeration takes place according to Ostwald ripening process [10]. The average grain size of CuO from FESEM was 45 ± 2 nm. Fig. 2c illustrates the FESEM images for PAni/CuO nanocomposite thin film. It can be noticed that the inorganic material (CuO) is grown on the fiber structure of organic material (PAni) forming a core/shell, where PAni is the core covered by CuO which acts as the shell [10]. The average grain size from FESEM was 29.6 ± 2 nm. Hybridization of the metal oxide with the conducting polymer will result in improved electrical conductivity of the material, in comparison with the low relative electrical conductivity of PAni and CuO nanostructures.

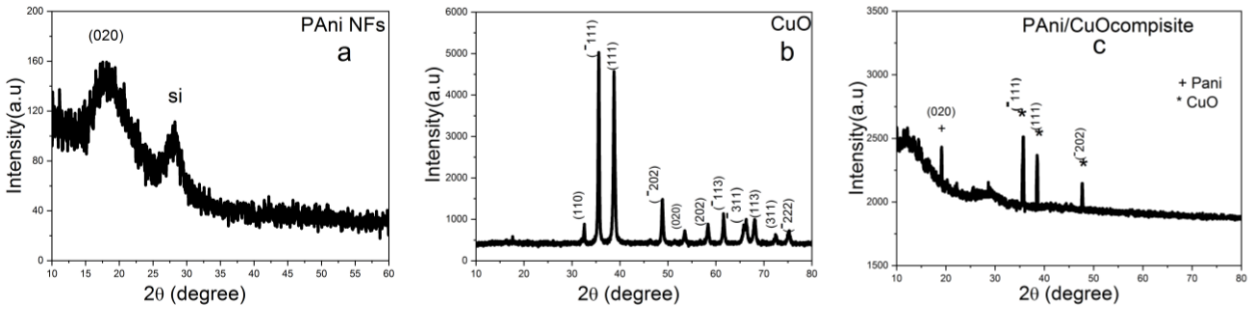

Fig. 1 – X-ray of PAni NFs (a), CuO thin film (b) and PAni/CuO composite (c)

Table 1 – Lattice constants of PAni NFs, CuO nanostructures and PAni/CuO composite

Sample	PAni NFs	CuO	PAni/CuO composite
D (nm)	11	21.8	64.7
Lattice constant (*a*) Å		4.692	4.4667
Lattice constant (*b*) Å		3.43	3.5674
Lattice constant (*c*) Å		5.134	5.3976

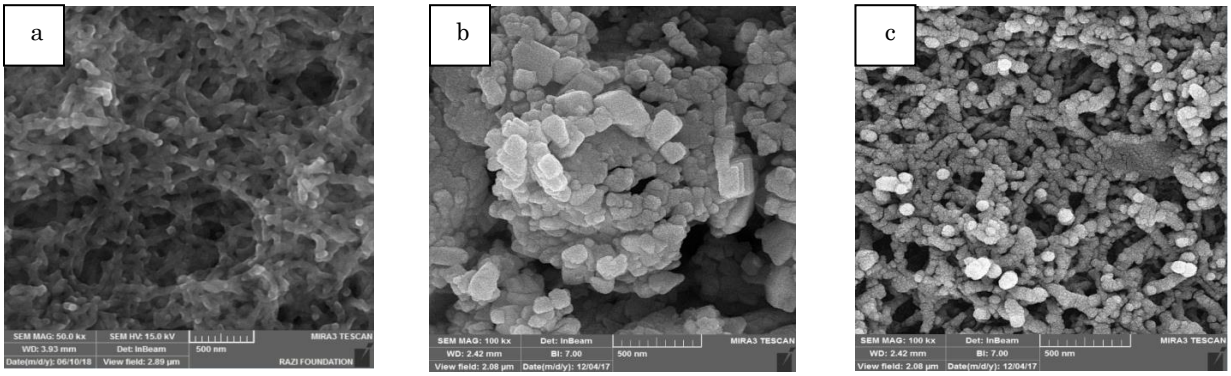

Fig. 2 – SEM images of PAni NFs (a), CuO (b) and PAni/CuO nanocomposite (c)

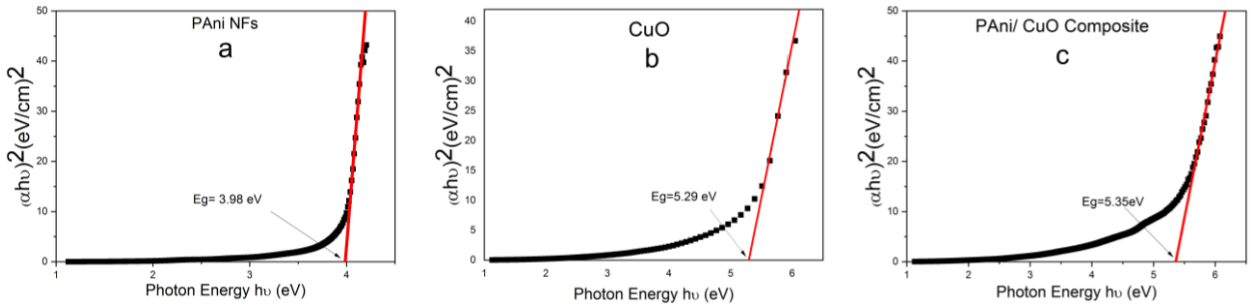

Fig. 3 – Energy gap for PAni NFs (a), CuO nanostructures (b) and PAni/CuO composite (c)

3.3 Optical Analysis

Optical absorption spectrum for PAni nanofiber solution in spectral series of 190-1100 nm was recorded by using UV-visible spectrophotometer. The analysis of the dependence of absorption coefficient on photon energy in the high absorption region was performed to get the complete information around the energy gap for the samples. The optical energy band gap E_g is given by Tauc's relation [13]:

$$\alpha h\nu = B\left(h\nu - E_g\right)^r, \qquad (2)$$

where a is the coefficient of absorption, $h\nu$ is the photon energy, E_g is the band gap, B is the constant and r depends on optical transitions. In this study, the direct band gap was determined by plotting a graph between $(ahv)^2$ and (hv) in eV, where the extrapolation of straight line to $(ahv)^2 = 0$ gives the value for the direct band gap of the material. It can be seen that the value ofthe band gap increases for PAni/CuO composite. This increase in the band gap may be related to the modification of structural properties for sample. The values of the energy gap for PAni NFs and CuO are 3.98 eV and 5.29 eV, respectively.

Moreover, the value of the energy gap was 5.35 eV for PAni/CuO composite, as shown in Fig. 3.

3.4 Photoconductivity Measurements

Photoconductivity of the fabricated PAni NFs, CuO nanostructures and PAni/CuO composite thin films on silicon wafers has been measured. The measurements include current-time (*I-t*) characteristics.

3.4.1. *I-t* Characteristics of PAni NFs Photoconductor Device

The current-time (*I-t*) characteristics are conducted with the wavelength of 250 nm. Fig. 4 shows the photoresponse for devices with time. Table 2 shows the sensitivity for PAni NFs, CuO and of PAni/CuO composites. When the light is turned on, the current increases, and after the light is turned off, the current returns to its original value. This process was repeated many times as shown in Fig. 4, and the rise and fall times in this process are less than 4 s for each state turn (on or off). From *I-t* figures, one can conclude that with mixing, the sensitivity is higher than that without mixing and found to be 220 %. PAni/CuO composites exhibit fast rise time of 0.32 s with full time of 0.41s, while the slow rise time of 0.67 s and 0.38 s was respectively observed for PAni NFs and CuO with full time of 3.32 s and 1.19 s respectively. This more enhancement in photoconductance can be attributed to the energy levels introduced by the addition of atoms lying in the corresponding band gap of PAni NFs. Such states served as "hopping" states and increased the excitation probability of an electron to the conduction band. Also it is noted that the current increased sharply upon exposure to UV light, and then exhibited hill-like behavior reaching the steady state. This behavior could be attributed to deep level defects that exist in the PAni/CuO nanostructure lattices which served as traps for photogenerated electrons. These results are in agreement with other studies [14, 15].

The responsivity of the PAni NFs based UV photodetector was obtained using equation [7]:

$$R(\lambda) = \frac{J_{ph}(\lambda)}{P_{inc}(\lambda)}, \qquad (3)$$

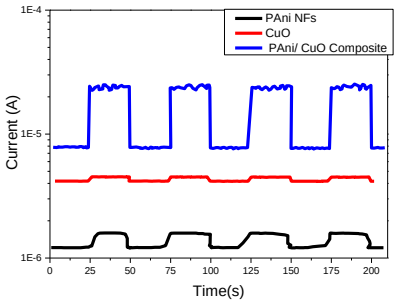

Fig 4 – Photoresponse time of samples as UV photodetector upon exposure to 250 nm

where $J_{ph}(\lambda)$ is the photocurrent density from the tested detector and $P_{inc}(\lambda)$ is the incident power density measured with the photodetectors as a function of wavelength. Fig. 5 displays the responsivity of the fabricated photoconductive detector as a function of wavelength for thin films. It is clear that there are several maximum responsivity values which are located at ~ 250, ~ 350 and ~ 475 nm [16]. The responsivity values at 250 nm were 0.25 and 0.65 A/W for PAni NFs and CuO respectively, the responsivity for PAni NFs mixed with CuO nanostructures films increases.

Table 2 – The sensitivity, rise time and fall time for all films

Sample	Rise time (s) at 250 nm	Fall time (s) at 250 nm	Sensitivity % at 250 nm
PAni NFs	0.67	3.32	30.8
CuO	0.38	1.19	8.5
PAni/CuO composite	0.32	0.41	220

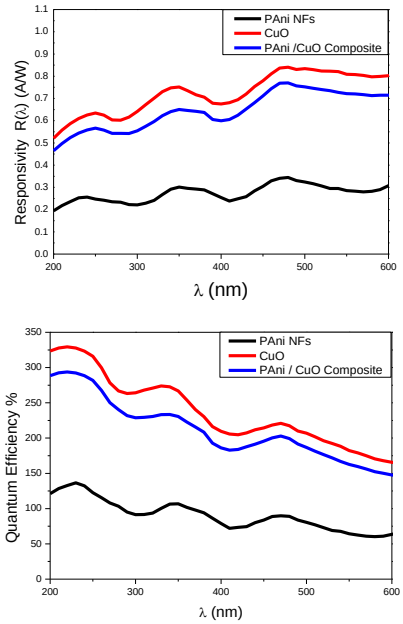

Fig 5 – The variation of spectral responsivity and QE with wavelength for PAni NFs, CuO and PAni/CuO composite

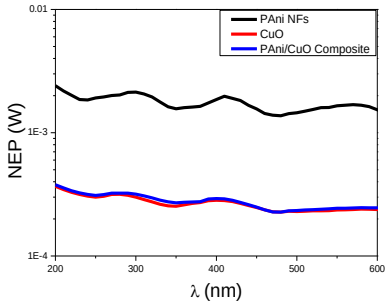

Fig 6 – NEP for PAni NFs, CuO and PAni/CuO composite

Table 3 – Result of PC detector for all films at 250 nm

Samples	$R(\lambda)$ (A/W)	QE (%)	NEP (W)
PAni NFs	0.25	130	0.0021
CuO	0.65	323	0.00031
PAni/CuO composite	0.56	288	0.00032

The quantum efficiency (QE) of the PAni NFs, CuO PAni/CuO composite photodetector was obtained using the relation [7]:

$$\eta(\lambda) = \frac{1240}{\lambda(nm)} xR(\lambda)x100\% . \quad (4)$$

One can see that PAni NFs and CuO nanostructures devices show QE of 130 and 323 % in UV region (250 nm) respectively, and for PAni/CuO composite it is larger than that for pure PAni NFs as shown in Fig. 5 and Table 3.

The noise-equivalent power (NEP) of the PAni NFs-based photodetector was obtained using the relation [7]:

$$\tau_r = \frac{2.2}{2\pi\Delta f} = \frac{0.35}{\Delta f}, \quad (5)$$

where I_n is the noise current (if noise from the dark current is the dominant contribution), so the noise current is given by:

$$I_n = \sqrt{\frac{4k_B T\Delta f}{R_d}}, \quad (6)$$

where R_d is the resistance of detector in the dark and Δf is the bandwidth which is given by:

$$\tau_r = \frac{2.2}{2\pi\Delta f} = \frac{0.35}{\Delta f}, \quad (7)$$

where τ_r is the rise time. The detection capability of the detector improves as the NEP decreases. NEP of the fabricated photoconductive detector was 0.0021, 0.00031 and 0.00032 W for PAni NFs, CuO PAni/CuO composite as shown in Fig. 6 and Table 3.

4. CONCLUSIONS

In this work, PAni NFs, CuO and PAni/CuO composite have been successfully synthesized by using hydrothermal method and deposited on silicon substrates by spin coating technique at room temperature with a thickness of about 325 nm. From the results, XRD proves that the PAni films have crystalline nature. CuO and PAni/CuO composites are polycrystalline in nature with monoclinic crystalline structures. The FESEM images of polyaniline clearly indicate that the polymer possesses nanofiber-like structure, whereas the CuO film has sponge-like shapes. The surface morphology of PAni/CuO composite is a nanofiber caped with inorganic material forming a core/shell, where PAni is the core covered by CuO which acts as a shell. The optical properties display that the direct electronic transition is allowed in the energy gap. The spectral response of PAni NFs, CuO and PAni/CuO composites was studied. The values of responsivity, specific detectivity and quantum efficiency of PAni/CuO composite are larger than those for pure PAni NFs and the current-time (I-t) characteristics show that the response has square pulse for UV-vis light region indicating faster response.

REFERENCES

1. I.M. Ali, A.M. Shano, N.A. Bakr, *J. Mater. Sci.: Mater. Electron.* **29** No13, 11208 (2018).
2. L.S. Carquigny, O. Segut, T. Patois, S. Lakard, *Metals* **9** No 5, 1371 (2015).
3. A. Mittiga, E. Salza, F, Sarto, M. Tucci, R. Vasanthi, *Appl. Phys. Lett.* **88** No 16, 163502 (2006).
4. D.W. Zhang, T.H. Yi, C.H. Chen, *Nanotechnology* **16** No 10, 2338 (2005).
5. E. Fortin, F.L. Weichman, *Can. J. Phys.* **40** No 12, 1703 (1962).
6. X. Zhu, K. Hou, C. Chen, W. Zhang, H. Sun, G. Zhang, Z. Gao, *High Performance Polymer.* **27** No 2, 207 (2015).
7. R.M. Al-Haddad, I.M. Ali, I.M. Ibrahim, *Eng. Tech. J.* **33** No 9, 1608 (2015).
8. A.D. Bhagwat, S.S. Sawant, Ch.M. Mahajan, *J. Nano- Electron. Phys.* **8** No 1, 01037 (2016).
9. K. Kannaki, P.S. Ramesh, D. Geetha, *Int. J. Sci. Eng. Res.* **3** No 9, 1 (2012).
10. S.M. Sathiya, G.S. Okram, M.A. Rajan, *Adv. Mater. Proc.* **2** No 6, 371 (2017).
11. D.M. Jundale, S.T. Navale, G.D. Khuspe, D.S. Dalavi, P.S. Patil, V.B. Patil, *J. Mater. Sci.: Mater. Electron.* **4** No 7, 19 (2013).
12. C.H. Srinivas, D. Srinivasu, B. Kavitha, N. Narsimlu, K. Siva Kumar, *IOSR J. Appl. Phys.* **1** No 5, 12 (2012).
13. D. Zhou, Y. Li, J. Wang, P. Xu, X. Han, *Mater. Lett.* **65** No 3, 3601 (2011).
14. D.M. Bubb, S.M. O'malley, C. Antonacci, R. Belmont, R.A. Mcgill, C. Crimi, *Appl. Phys.* **5** No 2, 1 (2004).
15. A. Ate, H. Zhu, X. Quan, H. Cai, X. Wang, Z. Tang, *Nano Sci. Nano Technol.* **7** No 3, 92 (2014).
16. T.L. Guidotti, *Int. Arch. Occup. Environ. Health* **66**, 153 (1994).

Властивості фотодетектора на основі наноструктур поліанілін/CuO, синтезованих гідротермальним методом

Ahmed M. Shano[1], Iftikhar M. Ali[2], Nabeel A. Bakr[3]

[1] *Bilad Alrafidain University College, Department of Radiological Techniques, Diyala, Iraq*
[2] *Department of Physics, College of Science, University of Baghdad, Baghdad, Iraq*
[3] *Department of Physics, College of Science, University of Diyala, Diyala, Iraq*

У роботі тонкі плівки (товщиною близько 325 нм) з нановолокнами PAni із чистого та змішаного оксиду міді успішно синтезуються на кремнієвих підкладках гідротермальним методом та технікою віджиму при кімнатній температурі. Досліджено структурні, поверхневі морфологічні, оптичні та фотопровідні властивості. Результати XRD показали, що плівки PAni мають кристалічну природу, наноструктурні композити CuO та PAni/CuO мають моноклінну полікристалічну структуру. Зображення FESEM чітко вказують, що PAni має структуру, подібну до нановолокон, в той час як плівка CuO має губчасту форму. Поверхневий морфологічний аналіз композиту PAni/CuO показує, що нановолокно, покрите неорганічним матеріалом, таким як CuO, є структурою типу ядро-оболонка. Оптичні характеристики показують, що в забороненій зоні допускається прямий електронний перехід. Значення забороненої енергетичної зони для нановолокон PAni та CuO складають відповідно 3,98 еВ та 5,29 еВ. Досліджено спектральний відгук нановолокон PAni, CuO та композиту PAni/CuO. Значення чутливості та квантової ефективності композиту PAni/CuO більше, ніж для чистих нановолокон PAni. Можна зробити висновок, що при змішуванні чутливість вища, ніж без змішування, і виявляється рівною 220 %. Композит PAni/CuO демонструє швидкий час нарощування 0,32 с при повній тривалості 0,41 с, тоді як для нановолокон PAni та CuO з повним часом 3,32 с та 1,19 с спостерігали повільний час нарощування рівний 0,67 с та 0,38 с.

Ключові слова: Поліанілін, Оксид міді, Гідротермальний метод, Спін покриття, Фотопровідність.